Experimental and Theoretical Study of Ketoconazole as Corrosion Inhibitor for Bronze in NaCl+Na₂SO₄ Solution

D.E. Millan-Ocampo[1], J.A. Hernandez-Perez[1], J. Porcayo-Calderon[1,] J.P. Flores-De los Ríos[2],
L.L. Landeros-Martínez[3], V.M. Salinas-Bravo[4], J.G. Gonzalez-Rodriguez[1,*], L. Martinez[5]

[1] Universidad Autonoma del Estado de Morelos, CIICAP, Av. Universidad 1001, 62209-Cuernavaca, Mor.,Mexico.
[2] Universidad Autónoma de Chihuahua, Facultad de Ingeniería. Circuito Universitario Campus II C.P. 31125 Chihuahua, Chih. México.
[3] Centro de Investigación en Materiales Avanzados S.C. Chihuahua, México
[4] Instituto Nacional de Energías Limpias, Av, Reforma 108, Temixco, Mor., Mexico
[5] Universidad Nacional Autonoma de Mexico, Instituto de Ciencias Fisicas, Av. Universidad S/N, 62209-Cuernavaca, Mor.,Mexico.
[*]E-mail: ggonzalez@uaem.mx;tel/fax

An antifungal, Ketoconazole, 1-[4-[4-[[(2R,4S)-2-(2,4-dichlorophenil)-2-(imidazol-1- ilmetil)-1,3-dioxolan-4-yl]metoxi]phenil]piperazin-1-yl]ethanol, has been evaluated as corrosion inhibitor for bronze in 3.5% M NaCl + 0.1M Na₂SO₄ solution with electrochemical techniques, including potentiodynamic polarization curves, linear polarization resistance and electrochemical impedance spectroscopy measurements at different concentrations and temperatures. Additionally, theoretical studies have been performed by using density functional theory (DFT) in order to know the relationship between the electronic properties of Ketoconazole and its inhibitive effect. Results show that Ketoconazole turned out to be a good mixed type of inhibitor, which is adsorbed in a physical way on to the metal surface by following a Langmuir type of adsorption isotherm. Inhibitor efficiency increases with time and inhibitor concentration, but it decreases with an increase in the temperature.

1. INTRODUCTION

Bronze is one of the first alloys developed by mankind, which is a common structural material, and corrosion resistant. Once the artefacts made of bronze are exposed to a corrosive environment such as atmosphere, seawater, or buried in soil, patina, i.e the corrosion products film, is formed. However, since there is an increased amount of pollutants into the atmosphere, more efficient ways for l

protection of bronze are needed when exposed to urban environment. One of the most commonly employed ways to protect metals against this attack is the use of corrosion inhibitors which in many cases are organic compounds containing N, P, S, and O due to their ability to adsorb on the metal surface [1, 2]. Some organic compounds include derivatives such as azoles [3-6], amines [7-10], amino acids [11, 12], plant extracts and natural products [13-17] and pharmaceutical compounds [18-26] which have been proved to be effective corrosion inhibitors. A cheap, easily available, non-toxic heterocyclic compound that is a derivative of imidazole is 1-[4-[4-[[(2R,4S)-2-(2,4-diclorophenil)-2-(imidazol-1-ilmethil)-1,3-dioxolan-4-yl]metoxi]phenil]piperazin-1-yl]ethanol, or Ketoconazole. The presence of heteroatoms such as N, O, and aromatic rings containing several π bonds could act as active sites for the adsorption process (Fig.1). Thus, the goal of this research work is to evaluate Ketoconazole as a corrosion inhibitor for bronze in NaCl + Na$_2$SO$_4$ solution, trying to simulate an urban-marine atmosphere.
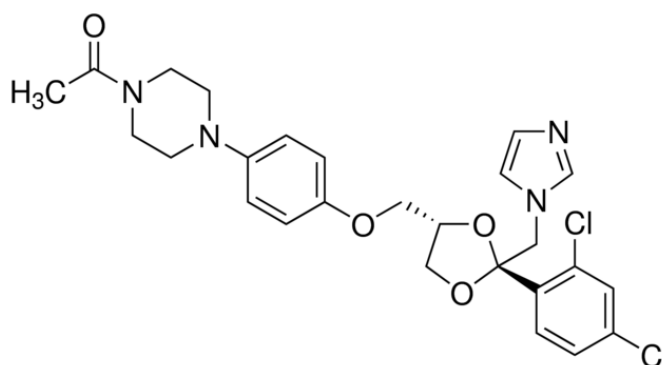

Figure 1. Chemical structure of Ketoconazole.

2. EXPERIMENTAL SOLUTION

2.1 Testing material

Testing material includes 6.00 mm diameter rods made of bronze with a chemical composition which includes 80 at. % Cu-7% Sn-7.5% Zn-4.5% Pb-1% Ni.

2.2 Aggressive solution

The used drug was supplied by a local pharmaceutical company. Aggressive solution was 3.5 wt. % NaCl + 0.1 M Na$_2$SO$_4$ prepared with analytical grade reagents and bi-distilled water. Concentrations used included 0, 5, 10, 25, 50, and 100 ppm at room temperature, (25 ^{0}C), 40 and 60 ^{0}C. Inhibitor was analyzed by using the fast Fourier infrared spectroscopy (FTIR) technique.

2.3 Potentiodynamic polarization curves

For the evaluation of Ketoconazole as corrosion inhibitor, potentiodynamic polarization tests, were performed with the use of a conventional three electrode electrochemical glass cell. A saturated

calomel electrode (SCE) was used as reference electrode, whereas a graphite was used as counter electrode. As working electrode, a piece of the bronze rode measuring 10 mm long, encapsulated in a polymeric resin were used. Before starting the tests, specimens were immersed in a 100 ml cell during 20 minutes until a stable free corrosion potential value (E_{corr}) was achieved. Experiments were carried out in a computer controlled potentiostat/galvanostat from ACM instruments. For polarization measurements potentials from -400 to +800 mV relative to the E_{corr} value were applied at a scan rate of 1 mV/s. Inhibitor efficiency was calculated with following equation:

$$I.E\ (\%) = \left(\frac{I_{corr} - I'_{corr}}{I_{corr}} \right) x\,100 \tag{1}$$

where I'_{corr} is the corrosion current density values with inhibitor and I_{corr} is the corrosion current density value without inhibitor, which were calculated with the Tafel extrapolation method.

2.4 Linear polarization resistance (LPR) measurements

For the LPR measurements, the same arrangement used for the polarization curves was used. Before starting the readings, specimen was immersed in the solution during 20 minutes until the E_{corr} value was stabilized. Following this, specimen was polarized from +15 to -15 mV around the E_{corr} value at a scan rate of 1 mV/s every 60 minutes during 24 hours.

2.5 Electrochemical impedance spectroscopy (EIS) mesurements

With the use of the same arrangement as described above, EIS experiments were carried out by applying an AC signal, 15 mV peak to peak and the frequency range was 0.05 - 30,000 Hz with the use of a PC4 300 Gamry potentiostat.

2.6 Quantum chemical studies

In order to find the effect of the inhibitor electronic structure on its inhibition properties, its geometry optimization, frontier molecular orbitals and local chemical reactivity calculations, the density functional theory (DFT) with the hybrid functional B3LYP was applied [27, 28] in combination with the 6-311G(d,p) Pople type basis set.

3. RESULTS AND DISCUSSION

3.1 Open circuit potential

The change in the open circuit potential (OCP) value with time for bronze in 3.5 % NaCl+0.1M Na_2SO_4 at different Ketoconazole concentrations is shown in Fig. 2.
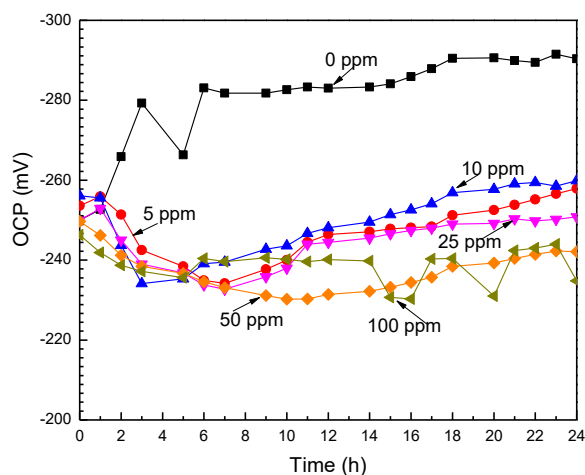
Figure 2. Effect of Ketoconazole concentration on the change of the OCP value with time for bronze in 3.5% NaCl+0.1M Na₂SO₄ solution.

When there is no inhibitor, the OCP value shifts towards nobler values as time elapses and it gets a stable value after a few hours of testing. On the other side, when Ketoconazole was added to the solution, the OCP value moves towards more active values during the first hours of testing, regardless of its concentration, but after this time, it moves to more positive values until a stable value is attained. During the whole testing time, the OCP values for the uninhibited solution was more positive than those obtained with the Ketoconazole. It has been reported that the shift in the OCP value towards more active values for Cu-base alloys is because any pre-formed film is being dissolved which makes the anodic dissolution reaction faster, while the movement in to nobler potential values is because a the formation of a protective copper oxide films is taking place [29].

3.2 Polarization curves

Polarization curves for bronze in 3.5 % NaCl+0.1M Na₂SO₄ at different Ketoconazole concentrations are shown in Fig. 3. It can be noticed that the shape of the curves is the same regardless the presence of Ketoconazole. In the anodic branch of the curve, there is a rapid increase in the current density value until a maximum, critical value is achieved, after which a decrease in the current density occurs, and a passive region is obtained. The critical current was observed at a potential value of -40 and -70 mV for uninhibited and inhibited solutions respectively. It has been reported [30] that the increase in the anodic current density is due to the formation of a film composed mainly either of copper hydroxide, cuprous oxide or cuprous chloride that protect bronze from a further dissolution. This films later on is dissolved, bringing an increase in the current density and the subsequent oxidation of copper into cupric ions [31, 32]. Oxygen reduction is observed in the cathodic branch as a limiting current density.
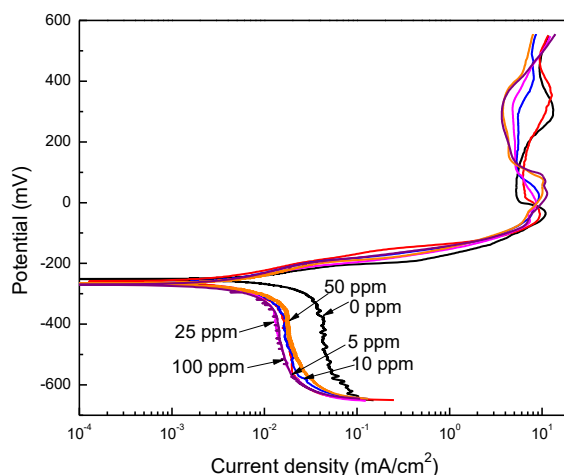
Figure 3. Effect of Ketoconazole concentration on the polarization curves for bronze in 3.5% NaCl+0.1M Na$_2$SO$_4$ solution.

This behavior has been reported by other authors [33, 34]. When Ketoconazole is added, the E$_{corr}$ value is practically unaffected, since it has a value of -252 mV for the uninhibited solution, whereas for the inhibitor containing solutions this value oscillated between -260 and -270 mV, as shown in table 1.

Table 1. Electrochemical parameters obtained from polarization curves for bronze in 3.5% NaCl+0.1M Na$_2$SO$_4$ solution.

C$_{inh}$ (ppm)	E$_{corr}$ (mV)	I$_{corr}$ (mA/cm^2)	β$_a$ (mV/dec)	I.E. (%)
0	-252	0.03	20	----
5	-268	0.015	50	50
10	-267	0.010	45	66
25	-269	0.015	40	50
50	-260	0.02	43	33
100	-270	0.02	45	33

The anodic current density value was marginally affected by the addition of Ketoconazole whereas the cathodic one was decreased, reaching its lowest value was obtained with the addition of 10 ppm of Ketoconazole. The corrosion current density value, I$_{corr}$, decreased with addition of Ketoconazole only up to 10 ppm, and it decreased when the inhibitor concentration increased. From table 1 it can be seen that the highest efficiency value was obtained with the addition of 10 ppm of Ketoconazole, and it decreases when the inhibitor concentration increases. Only a linear Tafel slope was observed in the anodic branch, with a value of 20 mV/dec for the uninhibited solution, whereas for

the inhibited solution it had values between 43 and 50 mV/dec. In the cathodic branch no linear slope was observed, only a limiting current density value due to the oxygen reduction reaction. It has been reported in the literature that if the free potential for the uninhibited solution is shifted more than 85 mV, then it can be said that the inhibitor is acting as an anodic type of inhibitor. On the other side, if the potential shift is lower than 85 mV, then it is acting as a mixed type of inhibitor. In our case, the maximum potential shift was lower than 20 mV, therefore we can say that Ketoconazole is acting as a mixed type of inhibitor.

3.3 Linear polarization resistance

The change in the R_p value with time for bronze in 3.5 % NaCl+0.1M Na_2SO_4 as a function of Ketoconazole concentration is shown in Fig. 4.
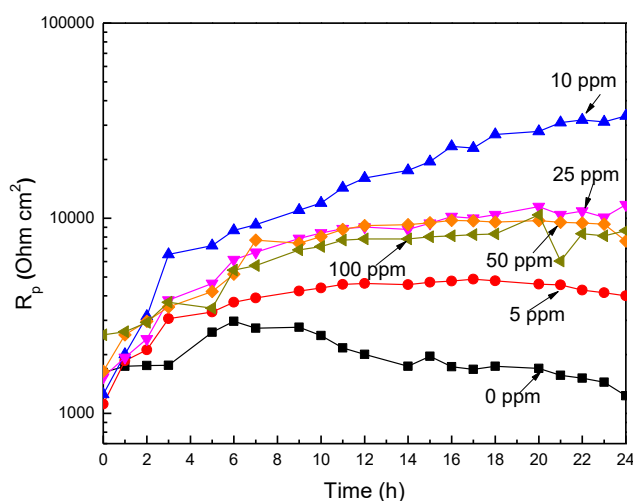

Figure 4. Effect of Ketoconazole concentration on the change of the R_p value with time for bronze in 3.5% NaCl+0.1M Na_2SO_4 solution.

In absence of inhibitor, the R_p value increases slightly during the first hours of testing, but after this time this value dropped markedly during the test, indicating an increase in the corrosion rate. As established above, the formation of cuprous oxide/hydroxide protect copper in natural fresh waters, but when chlorides are present, the formation of some unstable species containing copper and chloride increase the dissolution of copper [34, 35]. As soon as ketoconazole was added, the R_p value increased, obtaining its highest value with the addition of 10 ppm. A decrease in the R_p value was observed for inhibitor doses higher than 10 ppm, corroborating the results obtained by the polarization curves. In all cases, the R_p value in presence of Ketoconazole increased as time elapsed, due to the adsorption of Ketoconazole, and the covered surface by it increased. It has been established that organic inhibitors such as Ketoconazole are adsorbed on to the copper surface to form a protective film with the released

Cu^{2+} ions [36, 37]. The effect of Ketoconazole concentration on the inhibitor efficiency value with time is given in Fig. 5.
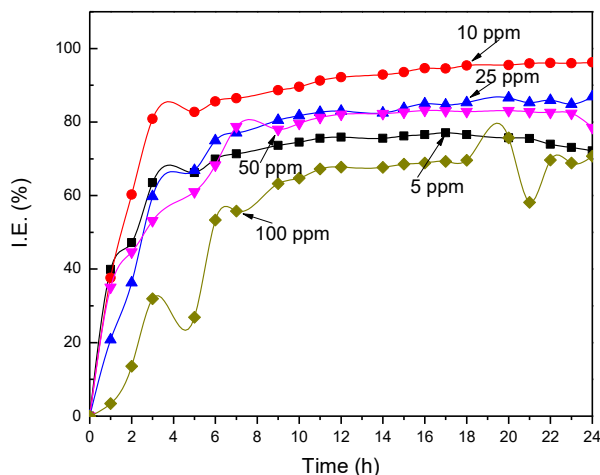

Figure 5. Effect of Ketoconazole concentration on the change of the inhibition efficiency value with time for bronze in 3.5% NaCl+0.1M Na$_2$SO$_4$ solution.
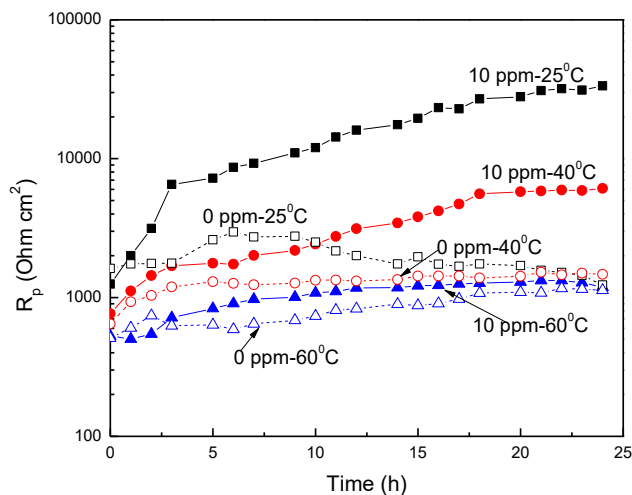

Figure 6. Variation on the R$_p$ value with time at 25, 40 and 60^{0}C bronze in 3.5% NaCl+0.1M Na$_2$SO$_4$ solution containing 0 and 10 ppm of Ketoconazole.

In this case, inhibitor efficiency was calculated by using equation:

$$E(\%) = \frac{R_{p,i} - R_{p,b}}{R_{p,i}} * 100$$

(2)

where R$_{p,i}$ and R$_{p,b}$ are the polarization resistance with and without inhibitor respectively. This figure shows that the inhibitor efficiency has its highest value in a Ketoconazole concentration of 10 ppm and it decreased when the inhibitor concentration increased. It increases in a slow fashion as time

elapses, and it never reaches a steady state value, but instead it keeps increasing during the whole period of testing. This increase is due to the formation of protective corrosion products on the surface covered by Ketoconazole which has been adsorbed on it.
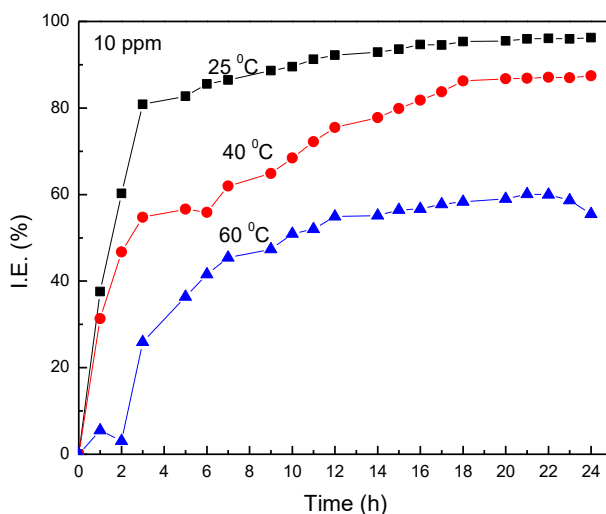

Figure 7. Variation of the inhibitor efficiency with time and temperature for bronze in 3.5% NaCl+0.1M Na$_2$SO$_4$ solution containing 10 ppm of Ketoconazole .

The effect of temperature on the R$_p$ value with time for bronze in 3.5% NaCl+0.1M Na$_2$SO$_4$ solution containing 0 and 10 ppm is shown in Fig. 6 whereas the efficiency values at these conditions are shown in Fig. 7. It is clear from Fig. 6 that regardless of the testing temperature, the addition of Ketoconazole increase the R$_p$ values and that in both the uninhibited and inhibited solutions, there is a decrease in the R$_p$ values when the testing temperature increased. The inhibitor efficiency values, Fig. 7, also decreased with an increase in the temperature, decreasing from a steady state value of 95 % down to 56% when the testing temperature increased from 25 ^{0}C at 60^{0}C. Thus, these tests show the degradation of the inhibitor with an increase in the testing temperature.

3.4 Electrochemical impedance spectroscopy tests

EIS data in both Nyquist and Bode formats at different Ketoconazole concentrations for bronze in 3.5% NaCl+0.1M Na$_2$SO$_4$ solution are given in Fig. 8. Nyquist diagrams, Fig. 8 a, display a single loop in the whole frequency values, which is indicative of a charge transfer controlled corrosion process. The loop shape did not change with the addition of the inhibitor, but the diameter loop increased with an increase in the Ketoconazole concentration, which is due to its adsorption, reaching its highest value with the addition of 10 ppm.
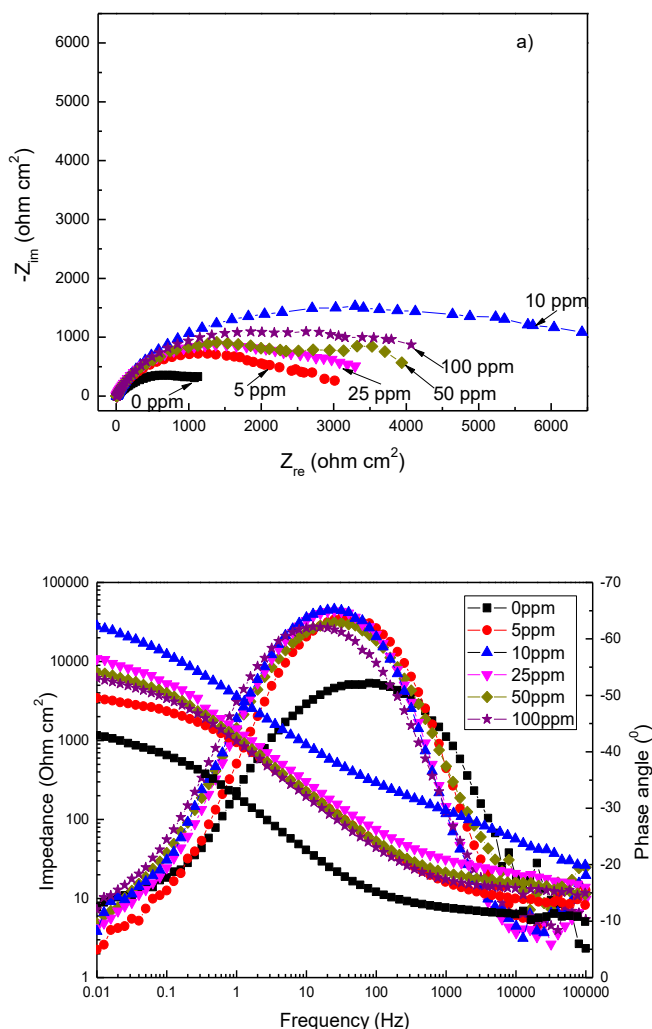
Figure 8. Effect of Ketoconazole concentration on a) Nyquist and b) Bode plots for bronze in 3.5% NaCl+0.1M Na$_2$SO$_4$ solution.

For Ketoconazole concentrations higher than 10 ppm, the loop diameter decreased. In another research work [38] similar results were obtained for mild steel in 1M HCl by using Ketoconazole, in similar concentrations, but in their case, the semicircle diameter increased with the inhibitor concentrations. Since the semicircles shown in Fig. 8 a are depressed, this is a phenomenon called "dispersion effect" due to the surface roughness and some other heterogeneities, and it has been reported for bronze and some other copper alloys in acid solutions with organic inhibitors [39, 40]. Bode diagrams, Fig. 8 b, show that the impedance modulus reaches its highest value with the addition of 10 ppm, whereas the angle phase reaches its highest value of -65^0 at this concentration also. Angle phase plots show the presence of a single peak for both, uninhibited and inhibited solutions, which shifts towards lower frequency values when the inhibitor was added to the solution. EIS data were fitted by the use of electric circuit shown in Fig. 9, where R$_s$ and R$_{ct}$ are the solution and charge

transfer resistance values respectively, and C_{dl} is the double layer capacitance. However, to take in to account the dispersion effects due to surface roughness and other surface heterogeneities, C_{dl}, is replaced by a constant phase element, CPE_{dl} instead of an ideal double layer capacitor. The magnitude of the impedance for the CPE, Z_{CPE}, can be calculated by using following expression [41]:

$$Z_{CPE} = = 1/[Y_0(\iota\omega)^n] \tag{3}$$

where Y_0 is the admittance, $\omega = 2\pi f$, f the frequency, and n is a physical parameter which gives some surface properties such as roughness, etc.. [41]. Electrochemical parameters obtained with the fitting can be used to calculate inhibitor efficiency values, I.E., with the use of following equation:

$$IE = 100 * \frac{R_{ct}^0 - R_{ct}}{R_{ct}^0} \tag{4}$$

where R_{ct}^0 y R_{ct} are the charge transfer resistance values with and without inhibitor respectively. An additional way to calculate the capacitance for the double layer is:

$$C_{dl} = (2\pi f_{max} R_{ct})^{-1} \tag{5}$$

where f_{max} is the frequency value where the maximum value of imaginary impedance is found.

Table 2. Electrochemical parameters obtained to fit EIS data for bronze in 3.5% NaCl+0.1M Na_2SO_4 solution using electric circuit shown in Fig. 9.

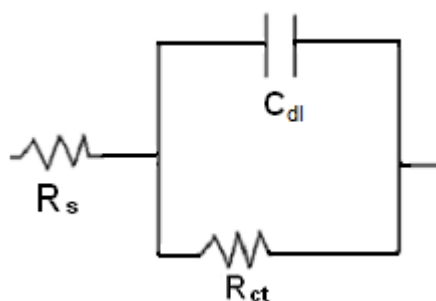| C_{inh} (ppm)	R_{ct} (ohm cm^2)	n	C_{dl} (μF cm^{-2})	I.E. (%)
0	1 147	0.85	350	----
5	3 654	0.91	274	68
10	30 650	0.95	212	96
25	11 689	0.92	280	90
50	7 918	0.89	300	85
100	6 735	0.83	371	82

Figure 9. Electric circuit used to fit de EIS data for bronze in 3.5% NaCl+0.1M Na_2SO_4 solution.

Obtained parameters by using circuit shown in Fig. 9 are listed in table 2, where it is clear that the R_{ct} and inhibitor efficiency values increase with increasing the Ketoconazole concentration, reaching their highest values with the addition of 10 ppm, and they decrease with higher doses of

Ketoconazole. Additionally, the double layer capacitance value, C_{dl}, decreases with the addition of Ketoconazole, obtaining its lowest value with the addition of 10 ppm. The C_{dl} value can also be calculated by using following equation:

$$C_{dl} = \varepsilon\varepsilon_0 A/\delta \tag{6}$$

where ε is the double layer dielectric constant, ε_0 the vacuum electrical permitivity, δ the double layer thickness, and A the surface area. Thus, when Ketoconazole is adsorbed on to the metal surface, their molecules, which have lower dielectric constant, replace the adsorbed water molecules causing the decrease in the C_{dl} value [42]. Another reason for the C_{dl} decrease is the decrease in surface area [43]. The n value has its lowest value, 0.85, for the blank, uninhibited solution, maybe due to the fact that the bronze surface is very rough for the corrosion effect. As the Ketoconazole concentration increases and the corrosion rate is decreased, the n value increases, due to a decrease in the metal surface roughness because the corrosion rate has been lowered.
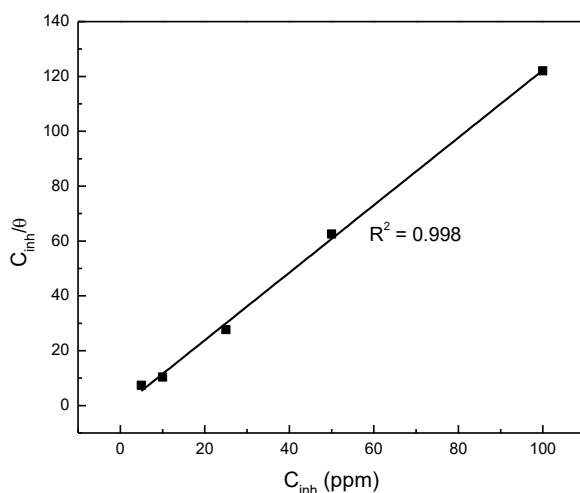
3.5 Adsorption isotherms

Figure 10. Langmuir adsorption for Ketoconazole at 25^0C.

Since it has been assumed that the decrease in the corrosion rate of bronze in 3.5 NaCl+0.1M Na_2SO_4 is due to the adsorption of Ketoconazole molecules on to the metal surface, in order to know the way it is adsorbed several adsorption isotherms were tested, but as it can be seen in Fig. 10, the best fit was obtained with the Langmuir type of adsorption isotherm. Data given in table 2 were used to calculate this isotherm. Langmuir adsorption isotherms is given by following equation:

$$\frac{C_{inh}}{\theta} = \frac{1}{K_{ads}} + C_{inh} \tag{7}$$

where K_{ads} is the equilibrium constant for the adsorption-desorption process constant, C_{inh} is the concentration of the inhibitor and θ is the surface coverage degree. The Ketokonazole adsorption Gibbs standard free energy was estimated by using the equation [41]:

$$\Delta G^{\circ}_{ads} = -RT \ lnK_{ads} \tag{8}$$

A value of is -37.25 kJ mol^{-1} for ΔG was obtained. A negative value for ΔG indicates that the adsorption of Ketoconazole molecules on to the bronze metal is spontaneous whereas a less negative value than -40 kJ mol^{-1} supports the idea that Ketoconazole adsorbs onto the bronze metal by a physical adsorption mechanism [42].

3.6 SEM micrographs

The appearance of corroded bronze specimens in 3.5 NaCl+0.1M Na$_2$SO$_4$ in absence and presence of 10 ppm of Ketoconazole are shown in the SEM micrographs given in Fig. 11.
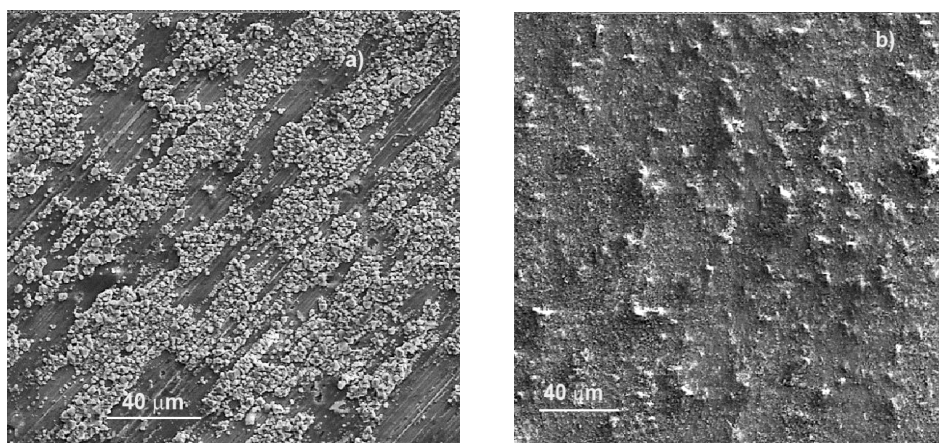

Figure 11. SEM Micrographs of bronze corroded in 3.5% NaCl+0.1M Na$_2$SO$_4$ solution containing a) 0 and b) 10 ppm of Ketoconazole at 25 ^{0}C.

In this figure, it can be seen that the film formed in the uninhibited solution contain defects such as porous and cracks, which allow the environment to ingress and attack the underlying metal. On the other hand, the formed film in the solution containing 10 ppm of Ketoconazole is much more compact, without evidence of defects such as porous or micro cracks, which is the responsible for the decrease in the corrosion rate of bronze.

3.7 FTIR study

In order to know the functional groups present in the Ketoconazole chemical structure, an FTIR spectrum was obtained, and it is shown in Fig. 12.
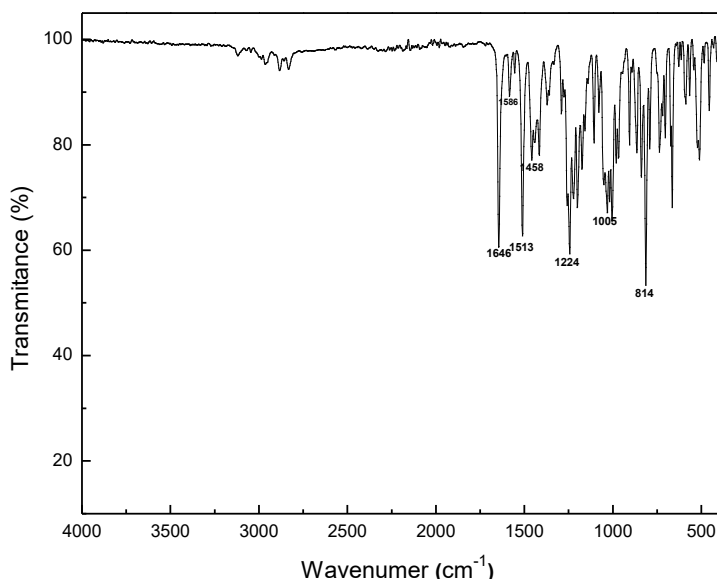
Figure 12. FTIR spectrum of Ketoconazole.

Several peaks are present in the spectrum, however, it shows intense absorption bands at 1647 cm^{-1} is due to a C=O link; the peaks shown at 1586 and 1005 cm^{-1} correspond to the amide (C-O) group, whereas the signal present at 1510 cm^{-1} was assigned to the C=C aromatic group; on the other hand, peaks exhibited at 1223 and 1200 cm^{-1} correspond to a tertiary amine, meanwhile the one shown at 1005 and 814 cm^{-1} is due to the C–Cl bond. The observed signal at 1646 corresponds to the C=O bond, whereas the one observed at 1513 cm^{-1} was assigned to the C=C functional group; the signal shown at 1458 cm^{-1} was assigned to the C=N bond, the one observed at 1224 cm^{-1} to the C-N bond [44]. Some of these groups, such as amines and amides have been widely used as corrosion inhibitors [7-12].

3.8 Quantum chemical studies

The molecular electronic structure together with its spatial molecular structure have a great influence in an inhibitor efficiency [45]. There are some chemical-quantum parameters that are related with the metal-inhibitor interaction such as E_{HOMO}, E_{LUMO}, ΔE, dipole moment (μ), electrophilicity, and the number of transferred electrons (ΔN). The molecule reactivity was investigated via analysis of the frontier molecular orbital. E_{LUMO} indicates the propensity of the molecule to accept electrons which increases with a decrease in the E_{LUMO} value. Conversely, the ability of that molecule to donate electrons increases with an increase in the E_{HOMO} value. The gap (ΔE), indicates the reactivity tendency of organic molecules to be adsorbed on to a metal surface, thus, the lower the ΔE value is, the higher is its tendency to be adsorbed on to a metal surface. Also, the tendency of inhibitor molecule to be accumulated on to the metal surface increases with a decrease in its dipole moment value. On the other hand, the electron-accepting capability of a molecule depends upon its electrophilicity index,. Normally, with the least value of hardness is expected to have the highest inhibition efficiency. The

inhibition efficiency resulting from electron donation depends upon the number of electrons transferred (ΔN). If $\Delta N < 3.6$, the inhibition efficiency increases by increasing electron-donating ability to the metal surface.   Optimized structure of Ketoconazole is shown in Fig.13, whereas the HOMO and LUMO diagrams are shown in Figs. 14 and 15 respectively.
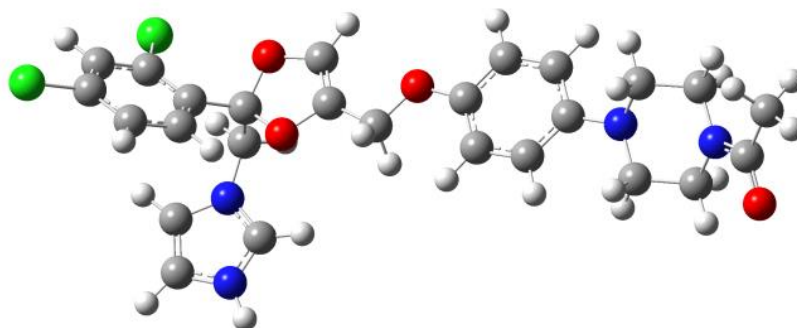

Figure 13. The optimized geometry of Ketoconazole molecule.
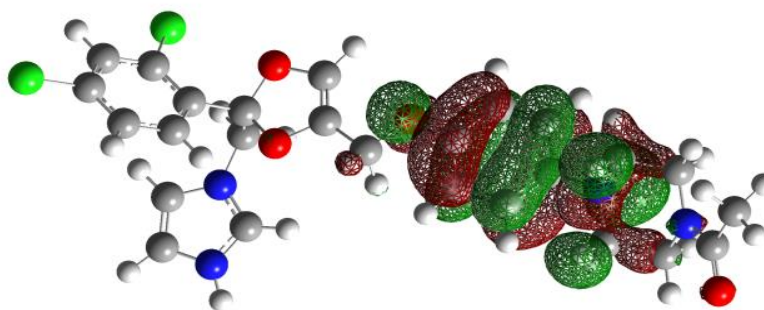

Figure 14. The highest occupied molecular orbital (HOMO) of Ketoconazole.

Mulliken charge densities were calculated for optimized structure of Ketoconazole in Fig. 16. Quantum chemical parameters are given in table 3. Fig. 14 shows that the HOMO region is mainly around benzene ring (carbon 25-30) and nitrogen 10, and therefore, these atoms are preferred sites for the donation of electrons to form bonds with vacant d orbitals of bronze and lone π-electrons.

Table 3. Quantum chemical parameters of Ketoconazole using gas phase B3LYP/6-31G (d,p)

Chemical Properties	Values
E_{HOMO} (eV)	-0.19623
E_{LUMO} (eV)	-0.04291
GAP (eV)	0.15332
Electronegativity (eV)	3.29
Hardness (eV)	2.01
Ionization Potential (eV)	5.30
Dipole Moment	2.314
Electrophilicity	2.69
Electron Affinity (eV)	1.28

Table 4. Mulliken charges on hetero-atoms.

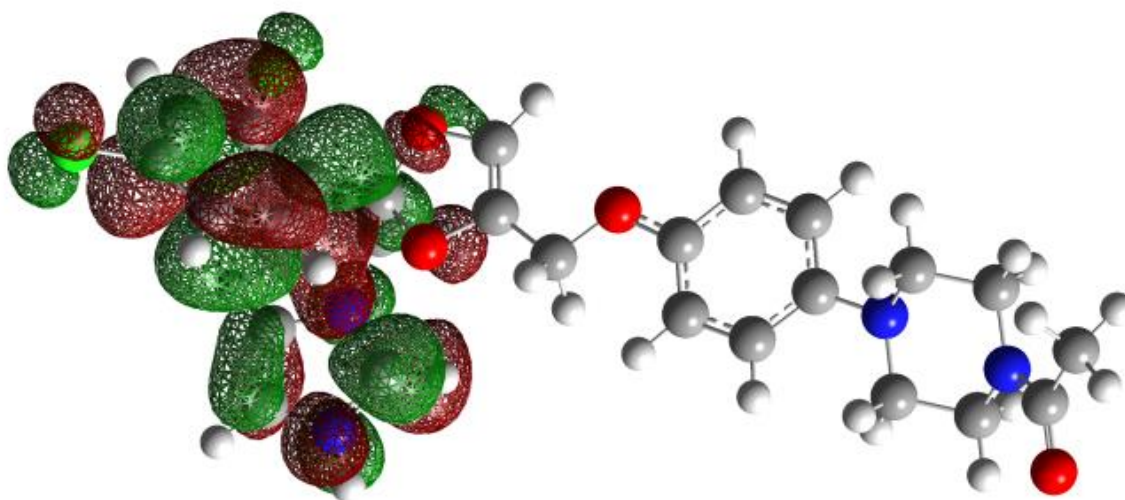| Mulliken charges					
3C	4N	7N	10N	13N	14O
0.103951	-0.000556	0.000249	-0.103439	-0.003643	0.012091

Figure 15. The lowest unoccupied molecular orbital (LUMO) of Ketoconazole.
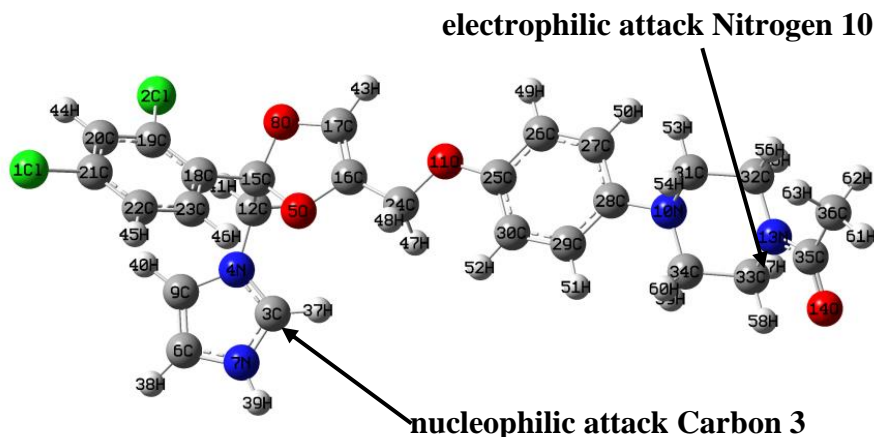

Figure 16. The nucleophilic and electrophilic attack in the Ketoconazole molecule using the Fukui function.

The low values for the dipolar moment and energy gap together with the high value for the hardness observed in table 3 indicates the great affinity for Ketoconazole to be adsorbed on to the bronze surface. The reaction of donating its electrons for an atom to the partially filled or vacant d orbital of the metal [47, 48] increases as the negative partial atomic charge of the adsorbed center increases. Figs. 15 and 16 together with results given in table 4 show that the most susceptible sites for electrophilic attack occur at the N4, N10 and N13 atoms, which indicates that these are the atoms with the highest tendency to donate electron pair to the metal surface [48].

Therefore, Ketoconazole can be adsorbed on to bronze metal surface by using the nitrogen atoms as active centers. The negative value of E_{HOMO} is an indication that Ketoconazole is physically adsorbed on to the bronze metal to form the protective corrosion products film. Additionally to this, the number of transferred electrons (ΔN) is lower than 3.6 which means that efficiency increases by increasing electron-donating ability to the metal surface. Since 80% of bronze corresponds to Cu, we can assume that the interaction mechanism between bronze and Ketoconazole molecule occurs through its interaction with copper. It has been proved [46] that Cu in H_2SO_4 solution becomes positively charged. In addition to this, in sulfuric acid, Ketoconazole can be easily protonated mainly in its nitrogen atoms [49]. The negatively charged SO_4 ions would be attached to the positively charged copper surface, so, the protonated Ketoconazole molecule could be attached to the copper surface by means of electrostatic interaction between SO_4 and protonated Ketoconazole. Once Ketoconazole has been adsorbed on to the copper surface, electrostatic interaction takes place by partial transference of electrons from the polar N atoms and the delocalized π electrons around the heterocyclic rings of Ketoconazole to the metal surface.

4. CONCLUSIONS

The results obtained from this work have proved that Ketoconazole is a good mixed type corrosion inhibitor for bronze in 3.5% NaCl + 0.1M Na_2SO_4 solution; its efficiency increased with an increase in its concentration up to 10 ppm, but after this value, inhibitor efficiency decreases. Efficiency also increases with elapsing time but decreases with an increase in the testing temperature. The decrease in the corrosion rate by Ketoconazole is due to its physical adsorption according to a Langmuir type of adsorption isotherm to form a protective corrosion products film. Ketoconazole can be adsorbed on to bronze surface by using its nitrogen and the π electrons of the aromatic ring atoms as active centers.

References

1. M.C. Bernard, E. Dauvergne, M. Evesque, M. Keddam and H. Takenouti, *Corros. Sci.,* 47 (2005) 663.
2. A. Igual Muñoz, J. García Antón, J.L. Guiñón and V. Pérez-Herranz*, Electrochim. Acta,* 50 (2004) 957.
3. E.M. Sherif and Su-Moon Park, *Electrochim. Acta,* 51 (2006) 6556.
4. M. Mihit, R.Salghi, S.El Issami, L.Bazzi, B.Hammouti, El.Ait Addi and S.Kertit, *Pigm. Resin. Technol.,* 35 (2006) 151.
5. X.R.Ye, X.Q.Xin, J.J. Zhu and Z.L.Xue, *Appl, Surf. Sci*., 307 (1998) 151.
6. J.C. Marconato, L.O. Bulhões and M.L. Temperini, *Electrochim. Acta,* 43 (1998) 771.

7.   E.M. Sherif, *Int. J. Electrochem. Sci.,* 7 (2012) 2832.
8.   E. Stupnisek-Lisac, A. Brnada and A.D. Mance, *Corros. Sci.,* 42 (2000) 243.
9.   H. Ma, S. Chen, L. Niu, S. Zhao, S. Li and D. Li, *J. Appl. Electrochem.*, 32 (2002) 65.
10. Maryam Ehteshamzadeh, Taghi Shahrabi and Mirghasem Hosseini, *Anti-Corrosion Methods and Materials,* 53 (2006) 296.
11. J.B. Matos, L.P. Pereira, S.M.L. Agostinho, O.E. Barcia, G.G.O. Cordeiro and E.D'Elia, J. *Electroanal. Chem.*, 570 (2004) 91.
12. G. Moretti and F.Guidi, *Corros. Sci.*, 44 (2002) 1995.
13. G. Khan, K. Md, S. Newaz, W.J. Basirun, H.B.M. Ali, F.L. Faraj and G.M. Khan*,   Int. J. Electrochem. Sci.,* 10 (2015) 6120.
14. A.. Fouda, K. Shalabi and A.A. Idress, *Green Chem. Let. Rev.*, 8 (2015) 17.
15. P.B. Raja, M. Fadaeinasab, A.K. Qureshi, A.A. Rahim, H. Osman, M. Litaudon and K. Awang, *Ind. Eng. Chem. Res.,* 52 (2013) 10582.
16. D.L. Lake, *Corros. Prevent. Contr.,* 15 (1988) 113.
17. A.Y. El-Etre, *J. Coll. Interf. Sci.*, 314 (2007) 578.
18. Sudhish Kumar Shukla and M. A. Quraishi, *J. Appl. Electrochem.*, 39 (2009) 1517.
19. L. Guo, S. T. Zhang, W. P. Li, G. Hu and X. Li, *Mater. Corros.,* 65(2014) 935.
20. M. Abdallah and B.A.Al Jahdaly, *Int. J. Electrochem. Sci.,* 10 (2015) 9808.
21. R. S. Abdel Hameed, E. A. Ismail, A. H. Abu- Nawwas and Hussin I. AL-Shafey, *Int. J. Electrochem. Sci.,* 10 (2015) 2098.
22.   S.K. Shukla and M.A. Quraishi, *Mater. Chem. Phys.*, 120 (2010) 142.
23. I. Ahamad, R. Prasad and M.A. Quraishi, *Corros. Sci.,* 52 (2010) 3033.
24. H. Tian, Y. F. Chengb, W. Li and B. Hou, *Corros. Sci.*, 100 (2015) 341.
25. D. Wang, B.Xiang, Y. Liang, S. Song and Chao Liu, *Corros. Sci.,* 85 (2014) 77.
26. I. Rotaru, S. Varvara, L. Gaina and L. M. Muresan, *Appl. Surf. Sci.,* 321 (2014) 188.

27.   A.D. Becke, *J. Chem. Phys.,* 98 (1993) 5648.

28. P.J. Stephens Devlin, F.J. Chabalowski and M.J. Frisch., *J. Phys. Chem.*, 98(1994) 11623.
29. K. Rahmouni, M. Keddam, A. Srhiri and H. Takenouti, *Corros. Sci.*, 47 (2005) 3249.
30. M. Benmessaoud, K. Es-salah, N. Hajjaji, H. Takenouti, A. Srhiri and M. Ebentouhami, *Corros. Sci.*, 49 (2007) 3880.
31. K. Es-Salah, M. Keddam, K. Rahmouni, A. Srhiri and H. Takenouti*, Electrochim. Acta*, 49 (2004)2771.
32. E. M. Sherif, A.M. El Shamy, M. M. Ramla and O.H. El Nazhawy, *Mater. Chem. Phys.*, 102 (2007) 231.
33. E M. Sherif and A. A. Almajid, *J. Appl. Electrochem.*, 40 (2010) 1555.
34. K.F. Khaled, *Mater. Chem. Phys.*, 125 (2011) 427.
35. B. Trachli, M. Keddam, A. Srhiri and H. Takenouti, *Corros. Sci.*, 44 (2002) 998.
36. I. Dugdale and J.B. Cotton, *Corros. Sci.*, 3(1963) 69.

37. F. Mansfeld, T. Smith and E.P. Parry,   *Corrosion, 27 (*1971) 289.
38. P. M. Nouri and M. M. Attar, *Chem. Eng. Comm.,* 203(2016) 505.
39. D.Q. Zhang, Q.R. Cai, X.M. He, L.X. Gao and G.D. Zhou, *Mater. Chem. Phys.*,112 (2008) 353.
40. M. Behpour, S.M. Ghoreishi, M. Salavati-Niasari and B. Ebrahimi, *Mater. Chem. Phys., 107*(2008) 153.
41. I.D. Raistrick, J.R. MacDonald, D.R. Franceschetti, *Impedance Spectroscopy Emphasizing Solid Materials and Systems*, John Wiley & Sons, New York, 1987.
42. A. Popova, E. Sokolova, S. Raicheva and M. Christov, *Corros. Sci.*, 45 (2003) 33.
43. F. Bontiss, M. Lagrence and M.Traisnel, *Corrosion,* 56 (2000) 733.
44. B. Karolewicz, A. Górniak, A.Owczarek, E.Zurawska-Płaksej, A. Piwowar and J. Pluta, *J. Therm. Anal. Calorim.,* 115 (2014) 2487.

45. H. Ashassi-Sorkhabi, B. Shaabani and D. Seifzadeh, *Electrochim. Acta,* 50 (2005) 3446.
46. R. Solmaz, E.A. Sahin, A. Doner and G. Kardas, *Corros. Sci.,* 53 (2011) 3231.
47. S. Martinez, *Mater. Chem. Phys.,* 77 (2002) 97.
48. S. Xia, M. Qiu, L. Yu, F. Liu and H. Zhao, *Corros. Sci*., 50 (2008) 2021.
49. I.B. Obot and N.O. Obi-Egbedi, *Surf. Rev. Lett.,* 15 (2008) 903.